Available online at www.sciencedirect.com
ScienceDirect
International Journal of Thermal Sciences 48 (2009) 26–33
International Journal of Thermal Sciences
www.elsevier.com/locate/ijts

Effects of a transverse, horizontal magnetic field on natural convection of a paramagnetic fluid in a cube

Tomasz P. Bednarz [a,*], Chengwang Lei [a], John C. Patterson [a], Hiroyuki Ozoe [b]

[a] *School of Engineering, James Cook University, Townsville, Queensland 4811, Australia*
[b] *Interdisciplinary Graduate School of Engineering Sciences, Kyushu University, Fukuoka, Japan*

Received 26 October 2007; accepted 10 March 2008

Available online 15 April 2008

Abstract

The present work is concerned with magnetic convection of a paramagnetic fluid in a cubic enclosure heated and cooled from the sidewalls. The influence of a 10-T transverse magnetic field on the convection mode of a paramagnetic fluid and the heat transfer rate was investigated numerically and experimentally, and compared with gravitational natural convection. The present study clearly shows that natural convection can be enhanced and the direction of the convective flow can be changed when using a strong magnetic field in terrestrial conditions.

Keywords: Natural convection; Magnetic convection; Numerical simulation; Flow visualization; Magnetic field

1. Introduction

Controlling convection phenomena in industrial and scientific applications is an interesting concept. However, before it can be applied, fundamental studies and experiments have to be carried out. Enhancements or suppressions of the convection phenomena and improvement of heat and mass transfer have been long-term research topics investigated by many researchers. In terrestrial conditions, the gravitational acceleration is constant and uniform everywhere, and thus controlling natural convection may not be simple. One of the simplest ways to provide additional body force to a working fluid is to rotate it [1]. Such a method has been extensively studied. However, there are difficulties in applying this technique in many real situations.

An alternative way of controlling the body force became feasible only a few years ago when it was possible to build high-temperature super-conducting magnets that operate in laboratory environments. Many new interesting phenomena have been reported concerning materials of low magnetic susceptibility. For instance, it is possible to levitate diamagnetic materials in terrestrial conditions. One of the most spectacular examples is the levitation of a famous frog (Larry) and the water droplets in the bore of a super-conducting magnet [2].

Quantitative treatment of fluid convection under magnetic fields was initiated by Bai et al. [3]. Braithwaite et al. [4] used magnetic fields both to enhance and suppress the Rayleigh–Benard convection in a solution of gadolinium-nitrate, and showed that the effect depends on the relative orientation of the magnetic force and the temperature gradient. Huang et al. [5] studied thermo-convection in a horizontal fluid layer by classical stability analysis. They created their own mathematical model to describe the convection of para- and diamagnetic fluids. Tagawa et al. [6] employed a procedure similar to the Boussinesq approximation and developed a simple model equation for convection resulting from a magnetic field. Most of the early works are summarized in a recent book by Ozoe [7].

The present work extends our previous investigations [8–11] carried out on natural convection of paramagnetic fluids in a cubic enclosure heated and cooled from two opposite walls. A transverse magnetic field is applied to the system and the magnetic force acts perpendicularly to the gravitational force. When the strength of the magnetic field is sufficient, the effect of gravity is negligible. Therefore, knowing how to control magnetic force makes it possible, for instance, to suppress the

* Corresponding author.
E-mail address: tomasz.bednarz@jcu.edu.au (T.P. Bednarz).

1290-0729/$ – see front matter
doi:10.1016/j.ijthermalsci.2008.03.011

Nomenclature

$\boldsymbol{b}$	magnetic induction (b_x, b_y, b_z)	T
b_0	reference magnetic induction, = 1–10 T	T
$\boldsymbol{B}$	dimensionless magnetic induction, $\boldsymbol{b}/b_0 = (B_x, B_y, B_z)$	
C	dimensionless momentum parameter for paramagnetic fluid, $= [1 + 1/(\beta\theta_0)]$	
$\boldsymbol{e}_z$	unit vector in the vertical direction	
g	gravitational acceleration	$\mathrm{m\,s^{-2}}$
l	length of the cubical enclosure, = 0.032 m	m
p	pressure	Pa
p_0	reference pressure, $= \rho_0\alpha^2/l^2$	Pa
P	dimensionless pressure, $= p/p_0$	
Pr	Prandtl number, $= \nu/\alpha$	
Ra	Rayleigh number, $= g\beta(\theta_h - \theta_c)l^3/(\alpha\nu)$	
t	time	s
t_0	reference time, $= l^2/\alpha = 10138.6$ s	s
T	dimensionless temperature, $= (\theta - \theta_0)/(\theta_h - \theta_c)$	
$\boldsymbol{u}$	velocity vector (u, v, w)	$\mathrm{m\,s^{-1}}$
u_0	reference velocity, $= \alpha/l$	$\mathrm{m\,s^{-1}}$
U	dimensionless velocity vector, $= \vec{u}/u_0 = (U, V, W)$	
X, Y, Z	$= x/l, y/l, z/l$	

Greek symbols

α	thermal diffusivity	$\mathrm{m^2\,s^{-1}}$
β	thermal expansion coefficient	$\mathrm{K^{-1}}$
γ	dimensionless gamma parameter, $= \chi_0 b_0^2/(\mu_m g l)$	
λ	thermal conductivity	$\mathrm{W\,m^{-1}\,K^{-1}}$
μ_m	magnetic permeability	$\mathrm{H\,m^{-1}}$
ν	kinematic viscosity	$\mathrm{m^2\,s^{-1}}$
θ	temperature	K
θ_0	average temperature, $= (\theta_h + \theta_c)/2$	K
θ_c	temperature of cooled wall	K
θ_h	temperature of heated wall	K
ρ	density	$\mathrm{kg\,m^{-3}}$
ρ_0	reference density at temperature θ_0	$\mathrm{kg\,m^{-3}}$
τ	dimensionless time, $= t/t_0$	
χ	mass magnetic susceptibility	$\mathrm{m^3\,kg^{-1}}$
χ_0	reference volume magnetic susceptibility at θ_0	
χ_m	volumetric magnetic susceptibility $= \chi \cdot \rho$	

Subscripts

0	reference point
c	cold
h	hot

influence of gravity and to study particular low gravity phenomena under terrestrial conditions. It is far more economical to conduct preliminary experiments on earth before sending space-craft to outer space to do experiments. Moreover, magnetic convection finds applications in crystal growth, mixing, material processing, etc., where the effects of convection may be undesirable. Therefore, these fundamental studies would be essentially worthwhile at the present time.

2. Experimental apparatus

Fig. 1 shows a schematic view of the experimental enclosure, the four walls of which were made of transparent Plexiglas. The left-hand-side copper plate was cooled by running water from a constant temperature circulator (RK20 KS LAUDA) and the right-hand-side copper plate was heated with rubber-coated nichrome wire connected to a DC power supply (Kikusui PAK 60-12A). The voltage and current of the nichrome wire were measured with two multi-meters respectively. The temperatures of the two copper plates were measured with six T-type thermocouples inserted into small and deep T.C. holes in each copper plate.

The enclosure was filled with an 80% mass aqueous solution of glycerol in which gadolinium nitrate hexahydrate $Gd(NO_3)_3{\cdot}6\,H_2O$ was dissolved to 0.8 mol/kg in order to make the working fluid paramagnetic. The fluid properties such as the magnetic susceptibility, density, viscosity and thermal expansion coefficient were measured and described in detail in [8,9], and thus those measurement techniques are not repeated here. Other properties are estimated for the 80% mass of aqueous solution of glycerol. Major properties of the working fluid are listed in Table 1.

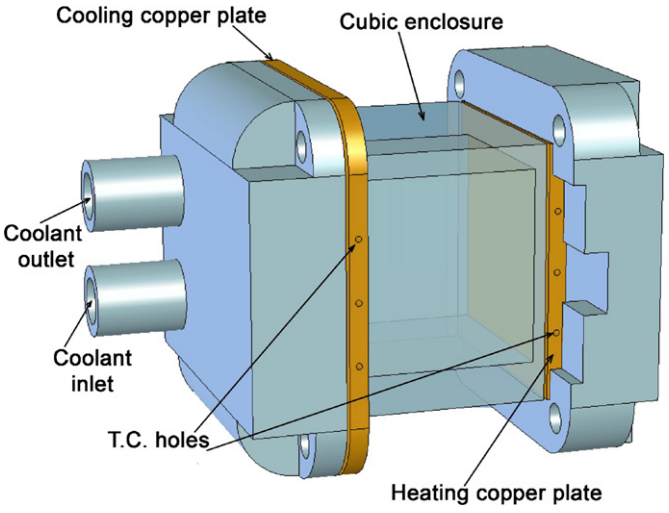

Fig. 1. Experimental apparatus. Internal dimensions of the cubic enclosure are 0.032 m on each side.

3. Flow visualization

In order to visualize and measure the temperature field, a very small amount of thermo-chromic liquid crystal slurry (KWN-20/25, Japan Capsular Products) was added to the working fluid. The color response of the liquid crystal slurry is presented in Fig. 2. The concentration of the slurry was adjusted for each experiment, and was in general less than 1 ppt. Quan-

Table 1
Important properties of the working fluid

Property	Value	Unit
α (Ref. [10])	1.01×10^{-7}	m^2/s
β	0.52×10^{-3}	$1/K$
λ (Ref. [10])	0.397	$W/(m\,K)$
μ	86.89×10^{-3}	$Pa\,s$
ν	5.9×10^{-5}	m^2/s
ρ	1463	kg/m^3
χ	23.09×10^{-8}	m^3/kg
Pr	584	–

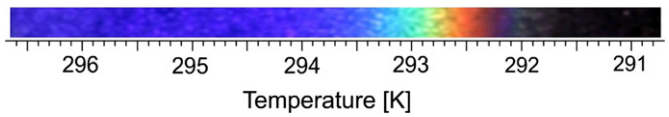

Fig. 2. Relation between temperature and hue illuminated by liquid crystal slurry (KWN-20/25 Japan Capsular Product Inc.).

titative temperature information was extracted non-invasively from the experimental photographs using the Particle Image Thermometry (PIT) technique. This was done using a calibrated hue versus temperature curve. With the calibration data, every pixel of the color photograph was transformed to a temperature value, and thus accurate experimental temperature maps were obtained. More details about this method can be found in [8,9].

Fig. 3 (a) and (b) shows the enclosure position in the experiment. The 10-Tesla super-conducting magnet was placed horizontally with the experimental model located just outside the bore of the magnet: the centre of the cube was at a distance of 0.233 m from the centre of the solenoids. Experimental photographs were taken at two middle cross-sections: one vertical and one horizontal, in two separate runs. In order to generate a vertical light-sheet, a mirror was placed above the enclosure to redirect the white light sheet coming from a projector lamp located at a distance of 3 m from the system to the downward direction. In this way, a vertical cross-section of the cube was illuminated, giving a color map of the temperature field. For photographing a horizontal cross-section, a horizontal light-sheet was directed towards the mid height of the enclosure, and the image of a color map was reflected by the mirror and then captured by a camera. All experimental images were taken by a Canon EOS 10D digital camera with a Canon EF 70-200 mm f2.8 IS lens after a steady state was attained for each case.

4. Numerical model

Corresponding numerical simulations have been carried out in order to compare numerical predictions with the experimental results. The numerical model for magnetic convection of a paramagnetic fluid is based on the work of Tagawa et al. [6]. It employs Curie's law under which the magnetic susceptibility of paramagnetic substances is inversely proportional to its absolute temperature. For not very large temperature differences, the magnetic susceptibility may be represented by a Taylor expansion and the magnetic force term in the momentum equation becomes proportional to the temperature T. When a temperature

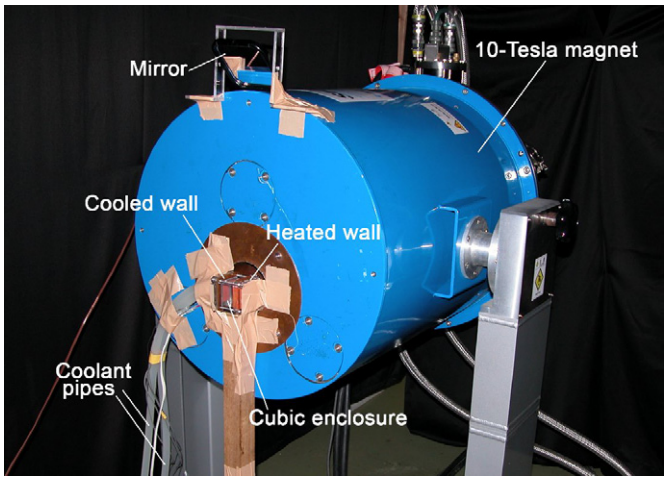

(a)

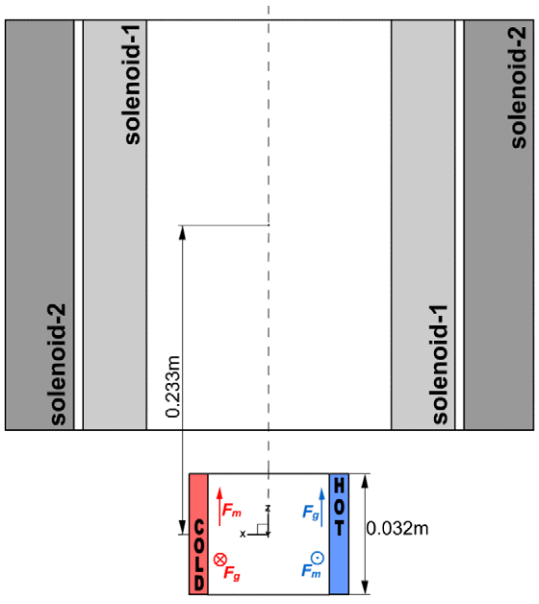

(b)

Fig. 3. (a) Photograph showing the enclosure position in the experiment. (b) Schematic top view of the experimental apparatus.

difference occurs in paramagnetic fluids, a magnetic buoyancy force is generated in the presence of a magnetic field. Examples of our previous computations using the same numerical model can be found in [8,9,11,12].

The non-dimensional forms of the governing equations are written as follows:

- Continuity equation

$$\nabla \cdot \boldsymbol{U} = 0 \tag{1}$$

- Momentum equation

$$\frac{D\boldsymbol{U}}{D\tau} = -\nabla P + Pr\nabla^2 \boldsymbol{U} + Ra\,Pr\,T\left[\boldsymbol{e}_z - \gamma\frac{C}{2}\nabla B^2\right] \tag{2}$$

- Energy equation

$$\frac{DT}{D\tau} = \nabla^2 T \tag{3}$$

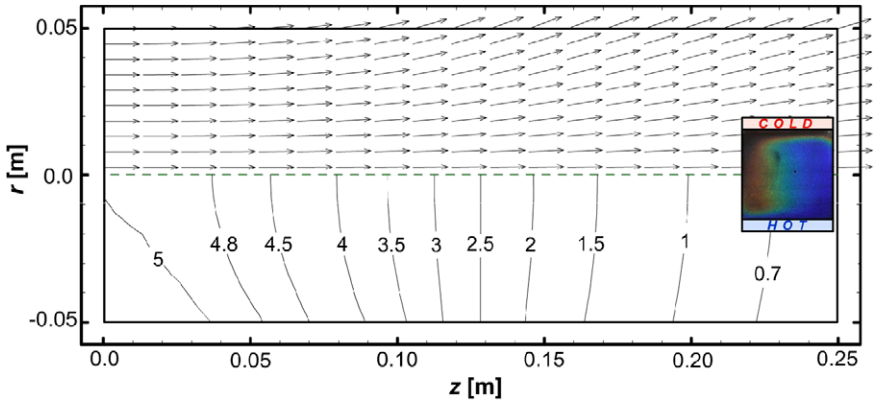

Fig. 4. Magnetic field distribution and location of the cubic enclosure in a magnetic field generated by a 10-Tesla super-conducting magnet when the magnetic induction is 5 T in the centre of the solenoids system.

- Momentum parameter for paramagnetic fluids

$$C = 1 + \frac{1}{\beta\theta_0} = 7.56 \tag{4}$$

- Prandtl number

$$Pr = \frac{\nu}{\alpha} = 100 \tag{5}$$

- Rayleigh number

$$Ra = \frac{g\beta l^3(\theta_h - \theta_c)}{\alpha\nu} = 28040 \cdot \Delta\theta \tag{6}$$

- Gamma parameter

$$\gamma = \frac{\chi_0 b_0^2}{\mu_m g l} = 0.586 \cdot b_0^2 \tag{7}$$

Normalization is done using the following formulae:

$$X = x/l, \quad Y = y/l, \quad Z = z/l$$
$$U = u/u_0, \quad V = v/u_0, \quad W = w/u_0$$
$$\tau = t/t_0, \quad P = p/p_0, \quad \boldsymbol{B} = \boldsymbol{b}/b_0$$
$$T = (\theta - \theta_0)/(\theta_h - \theta_c)$$

The boundary conditions for this system are given as follows:

$$U = V = W = 0 \quad \text{at all walls of the cube}$$
$$T = 0.5 \quad \text{at } X = -0.5$$
$$T = -0.5 \quad \text{at } X = 0.5$$
$$\partial T/\partial Y = 0 \quad \text{at } Y = -0.5, 0.5$$
$$\partial T/\partial Z = 0 \quad \text{at } Z = -0.5, 0.5$$

The initial condition is a state of linear conduction with

$$U = V = W = 0 \quad \text{and} \quad T = -X$$
$$\text{for } -0.5 \leqslant X \leqslant 0.5$$

All the above partial differential equations are approximated by a finite difference method. The HSMAC (Highly Simplified Marker and Cell) method is used to iterate mutually the pressure and velocity fields [13]. The number of meshes is chosen to be $40 \times 40 \times 40$. A grid dependency test for similar problems governed by the same set of equations was carried out in [11], which showed that the effect of the grid size was minor when compared with a $30 \times 30 \times 30$ mesh for the steady solution of the problem. The time-step was chosen to ensure numerical stability according to the CFL condition, and was fixed to $\Delta\tau = 10^{-7}$ in all subsequent numerical simulations.

Heat transfer through the cavity is measured by the Nusselt number. The average Nusselt number at the hot wall is computed as follows:

$$Nu = \frac{\int_{-0.5}^{0.5}\int_{-0.5}^{0.5}(\partial T/\partial X)_{X=-0.5}^{\text{convection}}\,dY\,dZ}{\int_{-0.5}^{0.5}\int_{-0.5}^{0.5}(\partial T/\partial X)_{X=-0.5}^{\text{conduction}}\,dY\,dZ} \tag{8}$$

Distribution of the magnetic field is computed using the Biot–Savart's law for a multi-coil system with two solenoids (as for our real 10-Tesla super-conducting magnet). Fig. 4 shows the computed distribution of the magnetic field when the magnetic induction in the centre of the solenoid system is set to 5 T. The vectors are normalized to unity in order to show clearly the direction of the magnetic induction, and the iso-lines represent their real magnitudes. The position of the experimental enclosure is also indicated in this figure. The strength of the magnetic field at that position is weak in comparison to that at the centre of the bore. However, it is strong enough to demonstrate the interaction of the magnetic buoyancy force with the gravitational buoyancy force.

5. Results and discussion

As indicated above, flow visualization was carried out with a 10-Tesla super-conducting magnet with the experimental model placed just outside the bore of the horizontally located magnet. In such a configuration, the magnetic force is acting in the perpendicular direction to the gravitational force and always attracts paramagnetic fluids. However, due to the variations of the magnetic susceptibility caused by temperature change (according to the Curie's law), cold fluid has a relatively larger value of the magnetic susceptibility and is attracted more when compared with hot fluid. Because the fluid is enclosed in a cavity and the continuity equation has to be satisfied, it always appears that relatively cold fluid is attracted to the magnet, and relatively hot fluid is repelled from the magnet, as can be seen

Table 2
Experimental parameters

Case	b_0 [T]	γ [–]	T_h [°C]	T_c [°C]	ΔT [°C]	Ra
F0	0	0	21.54	17.91	3.63	1.02×10^5
F5	5	14.650	21.51	17.93	3.58	1.00×10^5
F6	6	21.096	21.49	17.91	3.58	1.00×10^5
F7	7	28.714	21.42	17.92	3.50	9.81×10^4
F8	8	37.504	21.35	17.93	3.43	9.62×10^4
F10	10	58.600	21.18	17.92	3.26	9.14×10^4
T0	0	0	21.59	17.91	3.68	1.03×10^5
T5	5	14.650	21.40	17.91	3.49	9.79×10^4
T6	6	21.096	21.38	17.93	3.45	9.67×10^4
T7	7	28.714	21.30	17.95	3.35	9.39×10^4
T8	8	37.504	21.20	17.89	3.31	9.28×10^4
T10	10	58.600	21.07	17.94	3.13	8.78×10^4

Cases starting with F are experiments with photo taken from the front of cube, and those starting with T are experiments with photo taken from the top.

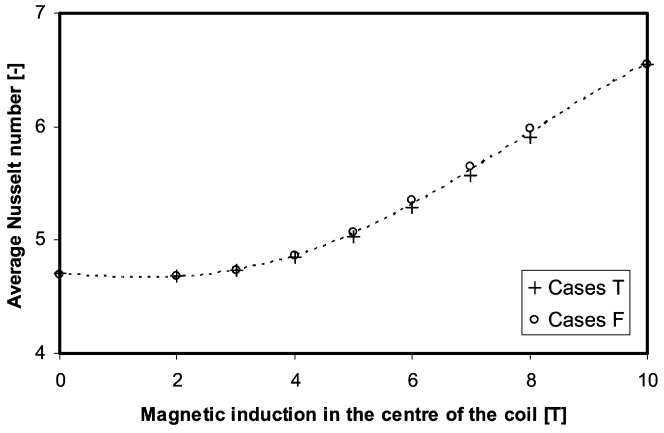

Fig. 5. The average Nusselt number computed on the hot wall for cases T and F.

later. Table 2 lists the experimental cases presented in this report. Two experimental runs were carried out for 0, 5, 6, 7, 8 and 10 T, respectively, and the photographs were taken at the vertical middle cross sections (cases F0–F10) and horizontal middle cross sections (cases T0–T10), respectively.

In Fig. 5, numerically computed average Nusselt numbers are plotted against magnetic induction measured in the centre of the coil. The average Nusselt numbers were not measured experimentally in this study, and thus direct comparison between the numerical and experimental results is not available. However, our previous reports [8,9,12] have confirmed that our numerical model is always in good agreement with experiments concerning magnetic convection. In this figure, circles and pluses represent numerical results for cases F and T, respectively. As seen in Fig. 5, the average Nusselt number increases with the magnetic induction, indicating enhancement of the convection by the transverse magnetic buoyancy force.

Qualitative comparisons between the experimental and numerical results are shown in Figs. 6, 7 and 8. Fig. 6 shows experimental photographs (on the left) of the horizontal middle cross-section and the corresponding numerical simulations (on the right) for cases T0, T5 and T10. Fig. 7 shows the experimental photographs (on the left) of the vertical middle cross-section and the corresponding numerical simulations (on the right) for cases F0, F5 and F10. It is worth noting that the experimental photographs in Fig. 6 were taken through the mirror, and the magnet position is the closest to the bottom of the photographs. Fig. 8 plots the force vectors, long-time streak lines and isothermal surfaces for cases T0, T5 and T10 (figures correspond to the mirror projection in Fig. 6).

At the magnetic induction of 0 T, the magnetic buoyancy force is not acting on the system, and thus pure gravitational natural convection can be observed. The force vectors observed in Fig. 8(a) (left figure) over the hot wall are directed upwards and those near the left-hand side cold wall are directed downward. In the upper part of the enclosure, relatively hot fluid prevails, in contrast to the lower part of the cube where the fluid is relatively cold as seen in Figs. 7 (upper figures) and 8(c) (left figure). As a result, a large roll is generated as seen from the long-time streak lines in Fig. 8(b) (left figure). Hot fluid first flows upwards along the heated wall and later along the top ceiling toward the cold wall. In the meantime, cold fluid flows downwards along the cold wall and finally along the bottom adiabatic wall toward the hot wall. Fig. 6 shows the temperature field in the horizontal middle cross-section. It is clear in this figure that the flow and temperature structures are symmetrical about the vertical mid cross-sectional plane along the transverse direction (refer to the upper figures in Fig. 6: the dashed line represents the symmetry line). Close to the adiabatic walls, three-dimensional effects due to the presence of the end-walls can be observed. This observation is also confirmed by the isothermal surfaces computed for the corresponding case in Fig. 8(c) (left figure). The average Nusselt number computed for case T0 is 4.712 and for case F0 is 4.696.

At the magnetic induction of 5 T, the magnetic buoyancy force acts together with the gravitational buoyancy force. As a result (refer to Fig. 8(a), middle figure), the previously-observed horizontally uniform force vectors along the heated and cooled walls at 0 T are now influenced by the magnetic field so that cold fluid is attracted toward the front adiabatic wall and hot fluid is repelled toward the rear adiabatic wall (the magnet is located at the front side of the cube). As a consequence, a twisted distribution of the temperature field is seen in Fig. 8(c) (middle figure). The long-time streak lines show that the convective rolls are skewed in comparison with the case at 0 T. The experimental isotherms observed in Fig. 7 (middle figures) are very similar to those at 0 T (upper figures). However, Fig. 6 shows that the symmetrical temperature structure observed without the magnetic force (at 0 T, upper figures) has been broken at the magnetic induction of 5 T (middle figures). It can be seen in Fig. 6 that the colder fluid is attracted toward the magnet (the magnet location is at the bottom of each photograph as shown by the sketch). The average Nusselt number computed for case T5 is 5.032 and for case F5 is 5.069.

At the magnetic induction of 10 T, the gravitational buoyancy force also acts together with the magnetic buoyancy force. However, the strength of the magnetic buoyancy prevails, and a nearly horizontal circulation of the fluid is observed. The symmetrical temperature structure observed in the horizontal cross-sectional plane for the case at 0 T (upper figures in Fig. 6) is destroyed completely, as can be clearly seen in Fig. 6 (lower fig-

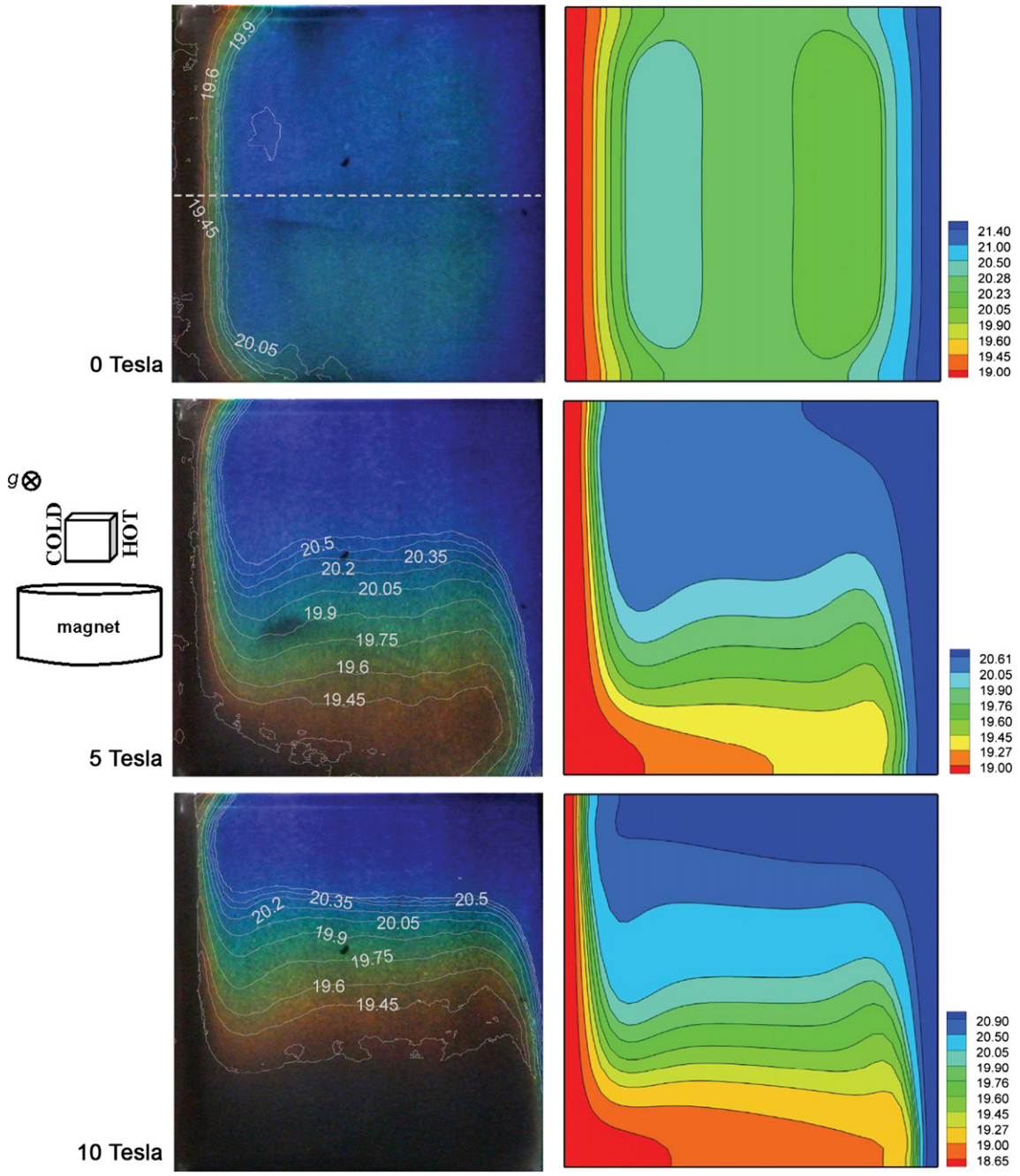

Fig. 6. Isotherms in a horizontal cross-section for cases T0, T5 and T10. Left: experiment + PIT, right: corresponding numerical simulations. The magnet location relative to the model enclosure is shown by the inserted sketch. The white dashed line drawn on the first photograph represents the symmetry line. For colors see the web version of this article.

ures). The relatively colder fluid (in brown/black colors) is "attracted" toward the magnet location and relatively warmer fluid is "repelled" from the magnet location. Fig. 8(b) (right figure) shows this flow behavior more clearly as a skewed and almost horizontal circulation. The gravitational force is insignificant compared with the magnetic force in this case. However, the effect of the gravitational buoyancy still can be seen in Fig. 8(c) (right figure) in which the relatively colder fluid falls downwards along the left-hand side cold wall and then horizontally along the front adiabatic wall. The force vectors observed in Fig. 8a (right figure) act almost horizontally. The calculated average Nusselt number for case T10 is 6.549 and for case F10 is 6.552, indicating enhancement of convection and thus heat transfer.

6. Conclusions

In this paper, the convection of a paramagnetic fluid under a strong magnetic field in a cubical enclosure has been investigated experimentally and numerically. The enclosure is placed horizontally with the rear adiabatic wall close to the magnetic coil. The experiment has been carried out for the cases with and

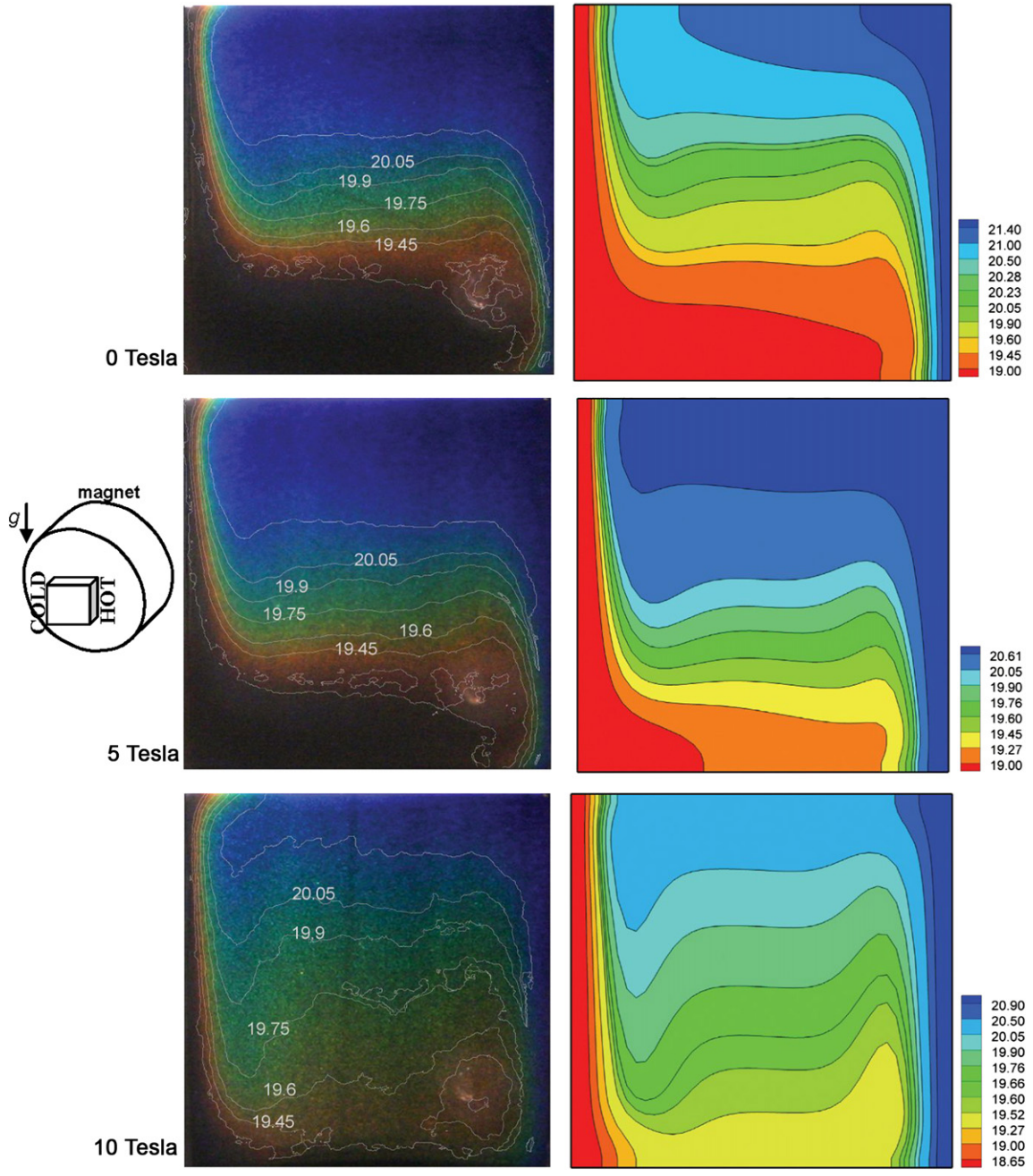

Fig. 7. Isotherms in a vertical cross-section for cases F0, F5 and F10. Left: experiment + PIT, right: corresponding numerical simulations. The magnet location relative to the model enclosure is shown by the inserted sketch.

without a magnetic field. The objective of this study is to show that gravitational convection can be overcome in terrestrial conditions with the application of a strong magnetic field. It has been demonstrated in this study that, at the magnetic induction of 10 T with the magnetic force acting perpendicularly to the gravitational force, an almost horizontal convective circulation is established in the enclosure. If an even stronger magnetic field is imposed, the gravity effect will become negligible. The accompanying three-dimensional numerical computation carried out for comparison purposes has verified the numerical model for the study of convection phenomena in a strong magnetic field.

In the present work, the enhancement of convection was successfully presented with the application of a strong magnetic field generated by a super-conducting magnet. It should be emphasized that by using a strong magnetic field we can also suppress or invert the usual gravitational convection with different combinations of the two main body forces (gravitational and magnetic buoyancy forces) that act together to drive thermo-magnetic convection of paramagnetic fluids. Therefore, this work is a natural extension of our previous investigations on this topic. For instance, paper [9] presents suppression of the convection to an almost conduction-like state. The cold fluid is there trapped by the magnetic buoyancy force acting in a hori-

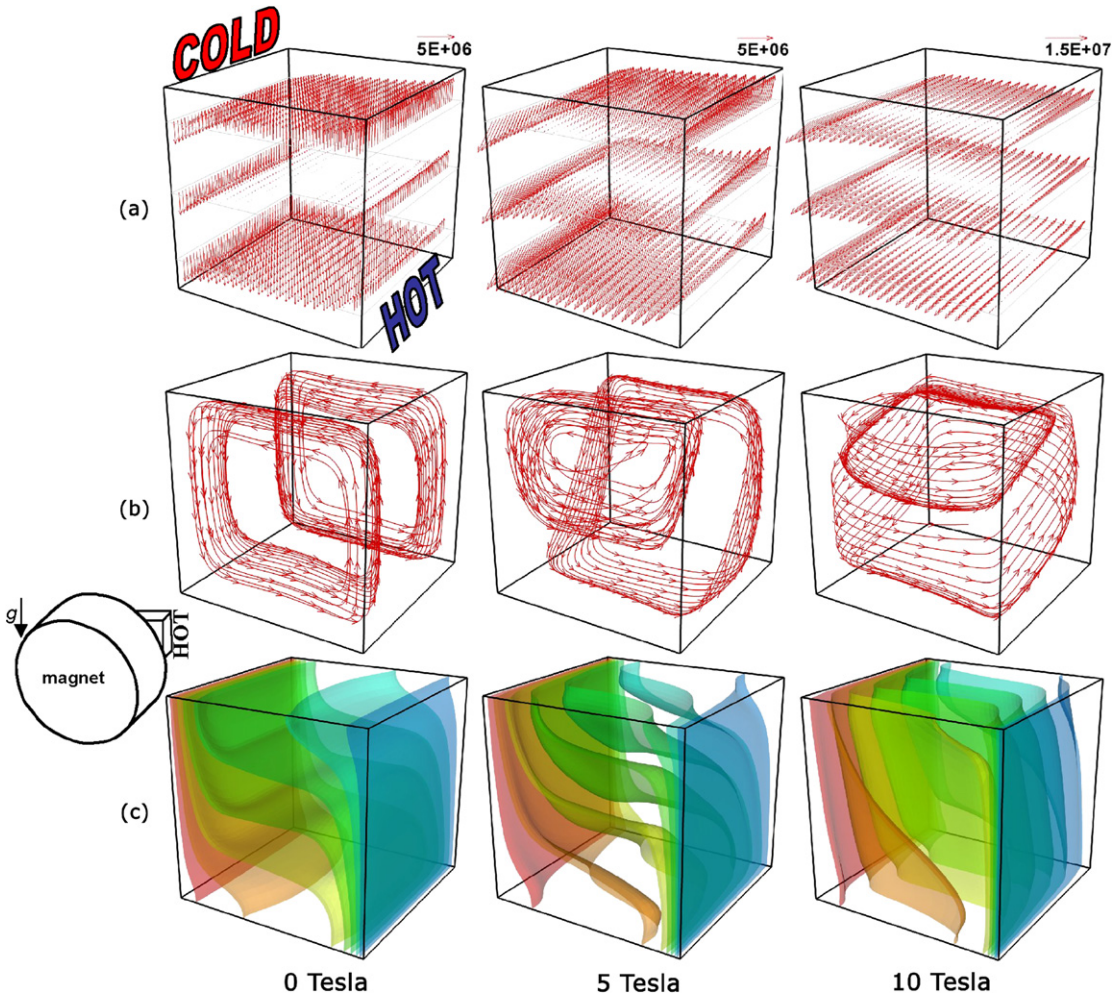

Fig. 8. Numerical results of cases T0, T5 and T10, (a) force vectors, (b) long-time streak lines, (c) isothermal surfaces. The magnet location relative to the model enclosure is shown by the inserted sketch.

zontal direction along the cold vertical wall situated close to the solenoid system. Paper [12] presents an inversion of the usual gravitational convection when the magnet is located above the enclosure. Additional examples of suppression or enhancement of the gravity effect on natural convection flows can be found in [6–8,11].

Acknowledgement

The authors are grateful to the Australian Research Council for its financial support.

References

[1] S. Chandrasekhar, Hydrodynamic and Hydromagnetic Stability, Dover Publications, 1961.
[2] M.D. Simon, A.J. Gaim, Diamagnetic levitation: flying frogs and floating magnets (invited), J. Appl. Phys. 87 (2000) 6200–6204.
[3] B. Bai, A. Yabe, N.I. Wakayama, Quantitative analysis of convection flow of nitrogen gas and air under magnetic field gradient, AIAA J. 37 (1999) 1538.
[4] D. Braithwaite, E. Beaugnon, R. Tournier, Magnetically controlled convection in a paramagnetic fluid, Nature 354 (1991) 667–673.
[5] J. Huang, D.D. Gray, B.F. Edwards, Thermoconvective instability of paramagnetic fluids in a nonuniform magnetic field, Phys. Rev. E 57 (1998) 5564–5571.
[6] T. Tagawa, R. Shigemitsu, H. Ozoe, Magnetizing force modelled and numerically solved for natural convection of air in a cubic enclosure: effect of the direction of the magnetic field, Int. J. Heat Mass Transfer 45 (2002) 267–277.
[7] H. Ozoe, Magnetic Convection, Imperial College Press, 2005.
[8] T. Bednarz, E. Fornalik, T. Tagawa, H. Ozoe, J.S. Szmyd, Experimental and numerical analyses of magnetic convection of paramagnetic fluid in a cube heated and cooled from opposing vertical walls, Int. J. Thermal Sci. 44 (2005) 933–943.
[9] T. Bednarz, E. Fornalik, H. Ozoe, J.S. Szmyd, J.C. Patterson, C. Lei, Influence of a horizontal magnetic field on the natural convection of paramagnetic fluid in a cube heated and cooled from two vertical side walls, Int. J. Thermal Sci. 47 (2008) 668–679, http://dx.doi.org/10.1016/j.ijthermalsci.2007.06.019.
[10] VDI-Wärmeatlas, VDI-Verlag, 1997.
[11] T. Bednarz, T. Tagawa, M. Kaneda, H. Ozoe, J.S. Szmyd, Numerical study of joint magnetisation and gravitational convection of air in a cubic enclosure with an inclined electric coil, Progress Comput. Fluid Dynamics 5 (2005) 261–270.
[12] T. Bednarz, E. Fornalik, T. Tagawa, H. Ozoe, J.S. Szmyd, Convection of paramagnetic fluid in a cube heated and cooled from side walls and placed below a superconducting magnet—comparison between experiment and numerical computations, Thermal Sci. Engrg. J. 14 (2006) 107–114.
[13] C.W. Hirt, B.D. Nichols, N. Romero, A numerical solution algorithm for transient fluid flows, Los Alamos Scientific Laboratory LA-5822, 1975.